Negative Pressure Vitrification of the Isochorically Confined Liquid in Nanopores

K. Adrjanowicz,[1,2] K. Kaminski,[1,3] K. Koperwas,[1,3] and M. Paluch[1,3]
[1]Institute of Physics, University of Silesia, ulica Uniwersytecka 4, 40-007 Katowice, Poland
[2]NanoBioMedical Centre, Adam Mickiewicz University, ulica Umultowska 85, 61-614 Poznan, Poland
[3]Silesian Center for Education and Interdisciplinary Research, ulica 75 Pulku Piechoty 1a, 41-500 Chorzow, Poland
(Received 24 August 2015; revised manuscript received 29 October 2015; published 22 December 2015)

Dielectric relaxation studies for model glass-forming liquids confined to nanoporous alumina matrices were examined together with high-pressure results. For confined liquids which show the deviation from bulk dynamics upon approaching the glass transition (the change from the Vogel-Fulcher-Tammann to the Arrhenius law), we have observed a striking agreement between the temperature dependence of the α-relaxation time in the Arrhenius-like region and the isochoric relaxation times extrapolated from the positive range of pressure to the negative pressure domain. Our finding provides strong evidence that glass-forming liquid confined to native nanopores enters the isochoric conditions once the mobility of the interfacial layer becomes frozen in. This results in the negative pressure effects on cooling. We also demonstrate that differences in the sensitivity of various glass-forming liquids to the "confinement effects" can be rationalized by considering the relative importance of thermal energy and density contributions in controlling the α-relaxation dynamics (the E_v/E_p ratio).

DOI: 10.1103/PhysRevLett.115.265702 PACS numbers: 64.70.P-, 62.50.-p, 77.22.Gm, 61.25.Em

The behavior of molecular liquids in confined geometry is much different from the bulk. Typical signatures of the "confinement effects" realized in uniform cylindrical nanopores (2D confining space) involve faster dynamics and the downward shift of the glass-transition temperature (T_g), as compared to the bulk [1–4]. However, for some of the glass-forming liquids (e.g., benzene or toluene) confined to very small nanopores, exceptions from this general trend were also reported [5]. The source of such dramatic changes is commonly discussed in terms of the competition between finite size effect and surface interactions [6–14]. Upon lowering the temperature, this leads to increased heterogeneity and divergence of the molecular dynamics (retarded mobility of the interfacial layer and the faster relaxation of the molecules in the center of the pores) [8,13,15].

Despite intensive studies, a thorough understanding of the behavior of confined glass-forming liquids is still missing. For example, it is intensely debated why the α relaxation in confined geometry suddenly becomes faster than the bulk, resulting in the crossover of the $\tau_\alpha(T)$ dependence from Vogel-Fulcher-Tammann (VFT) to Arrhenius law. It is also an open question as to what makes some of the glass-forming liquids and polymers show well-pronounced deviation from the bulk dynamics in nanopores, whereas the others are almost insensitive to nanoscale effects [9,16].

The motivation for this work is to look for a universal connection between the bulk and nanoscale dynamics that could help to address some of the most intriguing aspects of the glassy formation in confined geometry. This we postulate to be possible by taking into account the effect of pressure. Confinement at the nanometer length scale and bulk phase compression have already proven to be a source of unique information about the overall glassy behavior [13,17]. This results from the spectacular changes in the molecular packing and thermodynamic properties occurring in both cases. Strong indications that pressure effects should be taken into account when analyzing the behavior of soft matter in 2D confining space come from the similarities between numerous phenomena that are characteristic only for high pressure, but were observed also in the nanopores [18–23]. Theoretical calculation of the pressure tensor components (parallel and normal to the pore walls) has also indicated that simple fluids confined in the nanopores are subjected to hydrostatic pressure of either a positive or a negative sign [24–26]. Naturally, this can lead to a hypothesis of the important role of negative pressure in justifying the downward shift of T_g in nanopores.

Throughout the last decade, the importance of negative pressure effects in nanopores has received increasing attention [10,14,27,28]. No consensus has been reached so far, especially in the context of quantifying the magnitude of the negative pressure exerted on liquid while approaching the glass transition in confined geometry. It is experimentally inaccessible to measure the extent of negative pressure in pores. Therefore, it remains a challenge to provide convincing argumentation for or against the negative pressure hypothesis based on pure modeling, or estimates that employ mostly atmospheric pressure data.

In this study, we reexamine the role of negative pressure in vitrification of model glass-forming liquids confined to nanometer pores. To address this issue, we have to take a

close look at the dynamics of liquids in confined geometry, and the conditions that must be satisfied to enter the negative pressure region. As a next step, this was tested by using the temperature dependences of the isochoric relaxation times. Employing experimental results from high pressure enables us to show that, within the native nanopores, the density of the molecular liquid becomes frozen at the vitrification temperature of the interfacial layer, and this drives the negative pressure effects upon further cooling.

The materials under investigation include two model glass-forming liquids with different pressure sensitivities, salol ($dT_g/dP = 204$ K/GPa) and glycerol ($dT_g/dP = 35$ K/GPa) [29]. We have used commercially available anodized aluminum oxide (AAO) membranes as confining matrices (Synkera Technologies, Inc.). The prior treatment of the porous membranes and the infiltration procedure were carried out by following well-established methods reported in the literature [13]. The dielectric relaxation in confined geometry was followed by using the Novocontrol Alpha analyzer. The pore channels were aligned parallel with respect to the electric field. To avoid crystallization, our thermal protocol has involved cooling (with a rate of ~10–12 K/ min) of the melted sample down to the glassy state. Then, dielectric measurements were performed on heating with a rate of 0.5 K/ min.

The dynamics of glycerol and salol on increased pressure has been intensively studied over the years, even by some of us [29–36]. Therefore, the raw dielectric relaxation and pressure-volume-temperature (PVT) data can be found in the literature. For these measurements we have used a high-pressure Unipress system and a Gnomix dilatometer, respectively. The detailed description of the experimental equipment can be found in Ref. [29].

In Fig. 1(a) we present the temperature dependence of the α-relaxation time for salol in the bulk and confined within AAO nanopores of sizes varying from 100 to 13 nm. As can be seen, upon lowering the temperature and decreasing the pore sizes, the dynamics of salol becomes progressively enhanced in comparison to the bulk. Similar behavior was observed in silica nanopores and was related to the growing length scale of cooperativity, which at a certain temperature reaches the size of the spatial constraint [13,15]. On the other hand, we have recently demonstrated that the characteristic change in the $\tau_\alpha(T)$ dependence from the VFT to the Arrhenius law signifies vitrification of the molecules close to the pore walls. This phenomenon was interpreted in terms of a decoupling between the dynamics of the core and interfacial molecules [37], analogous to the decoupling phenomenon reported for ionic liquids (i.e., when the α relaxation is already frozen in at T_g but mobility of the ionic species is still active [38]).

Now, we wish to explore the possible link between deviation from the bulklike dynamics in confined geometry and the negative pressure effect. Vitrification of confined liquid under negative pressure requires the isochoric (fixed volume) conditions to be attained. This can actually favor the confining environment like uniform and unidirectional nanopores because, within a relatively narrow temperature range, the pore diameters are expected to be constant (as the thermal expansion coefficients of the porous material and the confined liquid are invariable to relatively small temperature changes). This could promote the isochoric conditions, and hence the negative pressure effects on cooling. Verifying this hypothesis requires us to show that (i) the $\tau_\alpha(T)$ dependences measured for salol in nanopores represent the isochoric curves, and (ii) they are located in the negative pressure zone. One of the most credible ways to test this is by using results from the high-pressure studies.

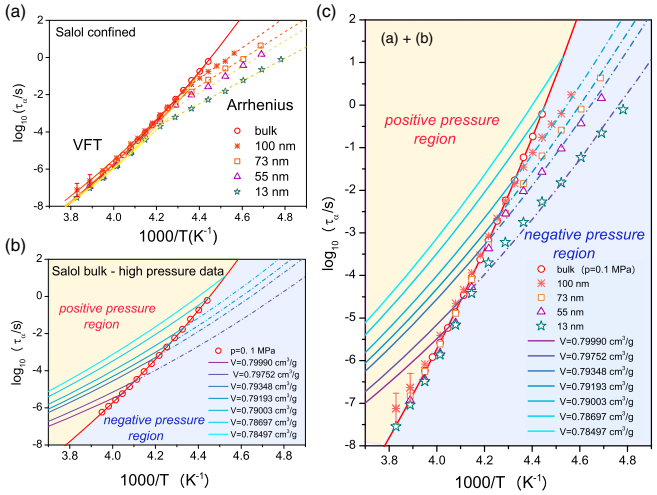

FIG. 1 (color online). Temperature dependence of the α-relaxation time for salol (a) in the bulk state and confined in AAO membranes of pore diameters from 100 to 13 nm, (b) along isochores (i.e., at constant volume conditions). Open circles denote the dependence of α-relaxation times at ambient pressure (in the bulk state). (c) The combined temperature dependences of the α-relaxation time for salol in pores and along isochores generated by using high-pressure data. The dash-dotted lines are an extrapolation of selected isochoric $\tau_\alpha(T)$ dependences from a positive range of pressure down to a negative pressure domain.

Figure 1(b) demonstrates the isochoric relaxation times for salol generated based on volumetric and high-pressure dielectric relaxation measurements. The temperature dependences of α-relaxation time along isochores were determined by parametrizing $V(T, p)$ and $\tau_\alpha(T, p)$ dependences to our recently derived equation of state for supercooled liquids [Eq. (9) in Ref. [39]] and the modified temperature-volume version of the Avramov model [40], respectively. Values of the fitting parameters are listed in Ref. [41].

As shown in Fig. 1(b), when the specific volume upon cooling is constant, the change of the relaxation time for salol is considerable weaker then along the isobar. Weaker temperature dependance of $\tau_\alpha(T)$ along isochores indicates that the contribution of the volume effects to the relaxation

dynamics of salol is significant. We have also noted that a relatively small change in the density produces pronounced variation of the isochoric $\tau_\alpha(T)$ dependence. Our observations can be quantified in a more accurate way by the E_V/E_p ratio, i.e., the ratio of the first derivatives of the $\tau_\alpha(T)$ dependences at constant volume and constant pressure [42],

$$\frac{E_V}{E_P} = \frac{R\left[\frac{\partial ln\tau_\alpha}{\partial(1/T)}\right]_V}{R\left[\frac{\partial ln\tau_\alpha}{\partial(1/T)}\right]_p}. \quad (1)$$

The lower (0) and upper (1) limiting values of the E_V/E_p ratio denote volume-dominated and purely thermally activated α relaxation, respectively. For salol, $E_V/E_p = 0.43 \pm 0.2$ [30], which indicates that the density and the thermal energy are equally important in governing the relaxation dynamics. In such a case, the appearance of even a small fluctuation in the density is able to alter the dynamics significantly.

The atmospheric pressure isobar presented in Fig. 1(b), together with the isochoric curves, separates the positive (measurable) range of pressure on the left from the negative pressure region on the right. Experimentally, we cannot access the isochoric relaxation times in the negative range of pressure. Nevertheless, they can still be estimated by extrapolating the corresponding $\tau_\alpha(T)$ dependences from the positive range of pressure. This we illustrate in Fig. 1(b) as dash-dotted lines. In the next step, we have used isochoric curves generated in this way to describe $\tau_\alpha(T)$ dependences in confined geometry, as demonstrated in Fig. 1(c). It is intriguing to note that the negative pressure isochores start to collapse with the confinement data at the range of temperature where the characteristic departure from bulklike dynamics occurs. In order to provide more convincing evidence for their similarity, we have compared slopes of the confined liquid data from the Arrhenius-like region and extrapolated to negative pressure isochores. The results of such a comparison can be found in Supplemental Material [43]. Therein, we have also demonstrated that it is possible to correctly describe the $\tau_\alpha(T)$ dependences in nanopores based on extrapolated isochoric data for other materials, like van der Waals liquid dimethyl phthalate ($E_V/E_p = 0.66$) [43]. Therefore, our observations indicate that supercooled liquids confined to nanopores indeed vitrify under negative pressure conditions enforced by the isochoric constraints.

While the modeling data by McKenna and co-workers [10] have indicated that isochoric conditions could appear only in the close vicinity of the glass-transition temperature, the results of the present study clearly demonstrate that the isochoric conditions in nanopores are reached far above it. Actually, the dynamics of confined salol enters the isochoric dependences at the temperature of the vitrification of the interfacial layer (i.e., more than 25–40 K above T_g). At this temperature, the density of the liquid becomes

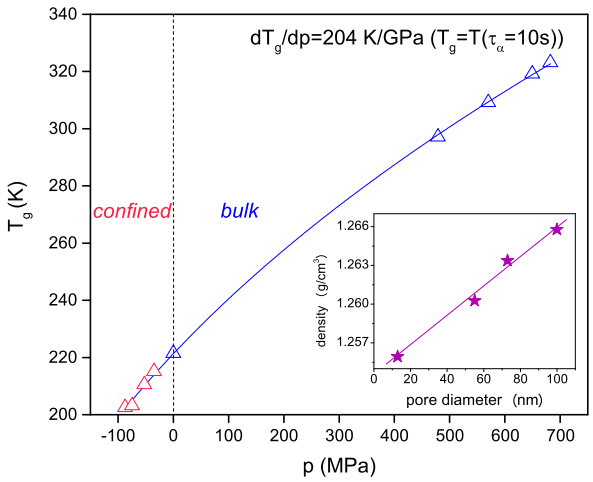

FIG. 2 (color online). Pressure dependence of the glass-transition temperature T_g for salol covering the experimental data from positive and negative ranges of pressure (confinement data). The solid line represents a fitting of the high pressure data to the Andersson-Andresson equation [Eq. (2)], while the inset shows the change of density as a function of pore size.

frozen, in contrast to the bulk sample from the atmospheric pressure. We imagine that starting from this point, the viscous liquid in the core must confront a very unusual situation. On one hand, it shows its natural tendency to decrease in specific volume with a lowering of the temperature. On the other, it is still strongly affected by the intermolecular interactions with the vitrified (immobile) interfacial layer. In such a situation, the appearance of negative pressure effects is able to save (stretch) the molecular system inside the nanopores from the collapse. Therefore, there is more volume available for molecules to move when compared to the bulk sample at the same temperature. In addition, the density of the confined liquid is expected to decrease with a lowering of the pore size, as illustrated in the inset of Fig. 2. This finding agrees with the results of recent PALS studies which show that the molecular liquid in the nanopores has, ironically, a higher effective free volume than in the bulk state [46].

To quantify the magnitude of the negative pressure exerted on salol in the pores, we have extrapolated the isochoric curves describing the $\tau_\alpha(T)$ dependences under confinement down to a dynamic glass-transition temperature. Typically, we refer to T_g as the temperature at which the α-relaxation time equals 100 s. However, for consistency with the high-pressure results, we have also assumed that the structural relaxation in the nanopores becomes frozen on a measurable time scale once τ_α reaches 10 s [30]. Values of the negative pressure at the corresponding isochoric glass-transition temperatures were estimated from the parametrized PVT data. The obtained dependence is presented in Fig. 2, together with high-pressure results described by using the Andersson-Andersson empirical relation [47],

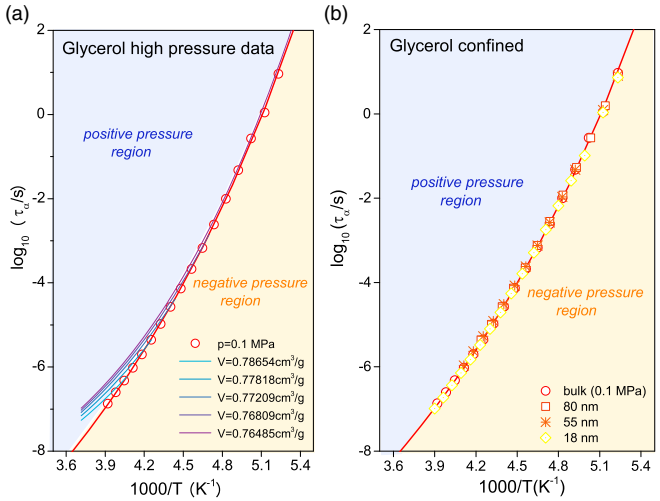

FIG. 3 (color online). Temperature dependence of the α-relaxation time for glycerol (a) along isochores and (b) confined to AAO nanopores of different sizes. Open circles denote $\tau_\alpha(T)$ dependence measured at 0.1 MPa (in the bulk state).

$$T_g = k_1\left(1+\frac{k_2}{k_3}P\right)^{1/k_2}. \quad (2)$$

For salol, the following set of fitting parameters was used: $k_1 = 221$ K, $k_2 = 2.5$, and $k_3 = 1080$ MPa [30]. It can be easily seen that extrapolating the $T_g(p)$ dependence from the positive to the negative region of pressure enables us to correctly describe the shift of T_g in the confined geometry.

Since the α relaxation in salol is fairly sensitive to density fluctuations (as classified by the E_V/E_p ratio), the freezing of the molecules interacting with the pore walls and the emergence of the isochoric conditions upon cooling are able to invoke a well-pronounced departure from the bulklike behavior. This we observe as a characteristic "kink" in the $\tau_\alpha(T)$ dependence. The question now arises, what if the α relaxation is controlled by the thermal energy, not the density fluctuations? Can we also expect in this case the enhancement of the dynamics on approaching T_g once the isochoric condition appears?

To address this question we have investigated the dynamics of glycerol confined in AAO nanopores. Glycerol is known to be a model glass-forming liquid with very weak sensitivity to pressure changes. The enthalpy ratio $E_V/E_p = 0.94$ points to an almost purely temperature-dominated dynamics [29]. The isochoric dependences determined for glycerol from the high-pressure data are presented in Fig. 3(a). In this case, the behavior of $\tau_\alpha(T)$ dependence along the isochores does not deviate significantly from the atmospheric pressure isobar. Furthermore, modifying the specific volume of supercooled glycerol by the same (or an even greater) magnitude as for salol produces considerably weaker changes in the isochoric relaxation time [41]. This is a clear sign that the appearance of the isochoric conditions and relatively small fluctuations in the density are not able to induce noticeable changes in the relaxation dynamics. Our interpretation corresponds with the bulklike behavior of the $\tau_\alpha(T)$ dependence for glycerol confined in AAO nanopores, as presented in Fig. 3(b). It is also consistent with the results of dielectric relaxation studies reported for glycerol confined in controlled-pore-glasses [16].

An interesting and unique observation coming from the current study is that by considering only the role of density fluctuations in controlling the α relaxation, we can rationalize the departure from the bulk (VFT) behavior in confined geometry. The E_V/E_p ratio can be used to rate deviation from the bulk dynamics appearing in a more (or less) pronounced manner for various glass-forming liquids. Furthermore, for those liquids which are fairly sensitive to the density variations, we are able to describe the temperature dependences of the α-relaxation time upon approaching the glassy state in a confined geometry by using the isochoric dependences from increased pressure. As we presume, vitrification of molecular liquids and polymers under isodensity and negative pressure conditions should also occur inside the unidirectional native silica nanopores. However, differences in the strength of the molecular interactions between the interfacial layer and the inner pore walls will probably tune the imposed isochoric conditions in a slightly different manner.

To summarize, the results of the present study have demonstrated that molecular liquids confined in native nanopores form a glass at constant volume under negative pressure. For the first time, we have also shown that the isochoric dependences from high pressure can be used to describe the behavior of α-relaxation time in confined geometry. Lastly, the magnitude of the departure from the bulklike dynamics in confined geometry can be rationalized and predicted by taking into account the relative importance of the density fluctuations in governing the α-relaxation dynamics (quantified by the E_V/E_p ratio). From a general perspective, our findings highlight the important role of pressure as a fundamental bridge between the dynamics of glass-forming liquids in the bulk and in nanoscale.

Financial support from the National Centre for Research and Development under research grant "Nanomaterials and their application to biomedicine," Contract No. PBS1/A9/13/2012, is gratefully acknowledged. K. K. is thankful for a financial assistance from the Polish National Science Centre within the program OPUS 9 (Project ID: 2015/17/B/ST3/01195).

[1] J.-Y. Park and G. B. McKenna, Phys. Rev. B **61**, 6667 (2000).
[2] C. L. Jackson and G. B. McKenna, J. Non-Cryst. Solids **131–133**, 221 (1991).

[3] J. A. Forrest, K. Dalnoki-Veress, J. R. Stevens, and J. R. Dutcher, Phys. Rev. Lett. **77**, 2002 (1996).

[4] C. L. Jackson and G. B. McKenna, Chem. Mater. **8**, 2128 (1996).

[5] D. Morineau, Y. Xia, and C. Alba-Simionesco, J. Chem. Phys. **117**, 8966 (2002).

[6] P. Pissis, D. Daoukaki-Diamanti, L. Apekis, and C. Christodoulides, J. Phys. Condens. Matter **6**, L325 (1994).

[7] J. Schuller, Y. B. Mel'nichenko, R. Richert, and E. W. Fischer, Phys. Rev. Lett. **73**, 2224 (1994).

[8] M. Arndt, R. Stannarius, W. Gorbatschow, and F. Kremer, Phys. Rev. E **54**, 5377 (1996).

[9] W. Gorbatschow, M. Arndt, R. Stannariu, and F. Kremer, Europhys. Lett. **35**, 719 (1996).

[10] S. Simon, J.-Y. Park, and G. McKenna, Eur. Phys. J. E **8**, 209 (2002).

[11] R. Richert, Annu. Rev. Phys. Chem. **62**, 65 (2011).

[12] C. Alba-Simionesco, B. Coasne, G. Dosseh, G. Dudziak, K. E. Gubbins, R. Radhakrishnan, and M. Sliwinska-Bartkowiak, J. Phys. Condens. Matter **18**, R15 (2006).

[13] *Dynamics in Geometrical Confinement*, edited by F. Kremer (Springer, New York, 2014).

[14] M. Alcoutlabi and G. B. McKenna, J. Phys. Condens. Matter **17**, R461 (2005).

[15] M. Arndt, R. Stannarius, H. Groothues, E. Hempel, and F. Kremer, Phys. Rev. Lett. **79**, 2077 (1997).

[16] M. Arndt, R. Stannarius, W. Gorbatschow, and F. Kremer, Phys. Rev. E **54**, 5377 (1996).

[17] *Molecular Dynamics of Glass-Forming Systems: Effects of Pressure*, edited by G. Floudas, M. Paluch, and K. Ngai (Springer-Verlag, Berlin, 2011).

[18] M. Beiner, G. Rengarajan, S. Pankaj, D. Enke, and M. Steinhart, Nano Lett. **7**, 1381 (2007).

[19] J.-M. Ha, J. H. Wolf, M. A. Hillmyer, and M. D. Ward, J. Am. Chem. Soc. **126**, 3382 (2004).

[20] L. D. Gelb, K. E. Gubbins, R. Radhakrishnan, and M. Sliwinska-Bartkowiak, Rep. Prog. Phys. **62**, 1573 (1999).

[21] J. Klein and E. Kumacheva, J. Chem. Phys. **108**, 6996 (1998).

[22] K. Kaneko, N. Fukuzaki, K. Kakei, T. Suzuki, and S. Ozeki, Langmuir **5**, 960 (1989).

[23] S. M. Shau Mien Ng, S. Ogino, T. Aida, K. A. Koyano, and T. Tatsum, Macromol. Rapid Commun. **18**, 991 (1997).

[24] Y. Long, J. C. Palmer, B. Coasne, M. Sliwinska-Bartkowiak, and K. E. Gubbins, Microporous Mesoporous Mater. **154**, 19 (2012).

[25] M. Sliwinska-Bartkowiak, H. Drozdowski, M. Kempinski, M. Jazdzewska, Y. Long, J. C. Palmer, and K. E. Gubbins, Phys. Chem. Chem. Phys. **14**, 7145 (2012).

[26] Y. Long, M. Sliwinska-Bartkowiak, H. Drozdowski, M. Kempinski, K. A. Phillips, J. C. Palmer, and K. E. Gubbins, Colloids Surf. **437**, 33 (2013).

[27] J. Zhang, G. Liu, and J. Jonas, J. Phys. Chem. **96**, 3478 (1992).

[28] A. Patkowski, T. Ruths, and E. W. Fischer, Phys. Rev. E **67**, 021501 (2003).

[29] C. M. Roland, S. S. Hensel-Bielowka, and M. Paluch, Rep. Prog. Phys. **68**, 1405 (2005).

[30] R. Casalini, M. Paluch, and C. M. Roland, J. Phys. Chem. A **107**, 2369 (2003).

[31] G. Dlubek, M. Q. Shaikh, K. Raetzke, F. Faupel, J. Pionteck, and M. Paluch, J. Chem. Phys. **130**, 144906 (2009).

[32] M. Paluch, R. Casalini, S. Hensel-Bielowka, and C. M. Roland, J. Chem. Phys. **116**, 9839 (2002).

[33] M. Paluch, S. Rzoska, P. Habdas, and J. Ziolo, J. Phys. Condens. Matter **8**, 10885 (1996).

[34] S. Pawlus, M. Paluch, J. Ziolo, and C. M. Roland, J. Phys. Condens. Matter **21**, 332101 (2009).

[35] C. Dreyfus, A. L. Grand, J. Gapinski, W. Steffen, and A. Patkowski, Eur. Phys. J. B **42**, 309 (2004).

[36] R. L. Cook, H. E. King, C. A. Herbst, and D. R. Herschbach, J. Chem. Phys. **100**, 5178 (1994).

[37] K. Adrjanowicz, K. Kolodziejczyk, W. K. Kipnusu, M. Tarnacka, E. U. Mapesa, E. Kaminska, S. Pawlus, K. Kaminski, and M. Paluch, J. Phys. Chem. C **119**, 14366 (2015).

[38] F. S. Howell, R. A. Bose, P. B. Macedo, and C. T. Moynihan, J. Phys. Chem. **78**, 639 (1974).

[39] A. Grzybowski, K. Grzybowska, M. Paluch, A. Swiety, and K. Koperwas, Phys. Rev. E **83**, 041505 (2011).

[40] R. Casalini, U. Mohanty, and C. M. Roland, J. Chem. Phys. **125**, 014505 (2006).

[41] For salol, $T_0 = 273.15$ K, $P_0 = 0.1$ MPa, $A_0 = 0.81625$ cm^3/g, $A_1 = 0.00061635$ cm^3/(gK), $A_2 = 0.00000208707$ cm^3/(gK^2), $B_{T_0}(P_0) = 2557.74147$ MPa, $b_2 = 0.0049$ K^{-1}, $\gamma_{\mathrm{EOS}} = 9.55331$, $\log_{10}(\tau_0/\mathrm{s}) = -12.93915$, $A = 216.05871$ cm$^{3\gamma}$ g$^{-\gamma}$ K, $D = 2.89848$, $\gamma = 5.04543$. For glycerol, $T_0 = 100$ K, $P_0 = 0.1$ MPa, $A_0 = 0.72872$ cm^3/g, $A_1 = 0.000351965$ cm^3/(gK), $A_2 = 0.000000109899$ cm^3/(gK^2), $B_{T_0}(P_0) = 4666.79$ MPa, $b_2 = 0.00193$ K^{-1}, $\gamma_{\mathrm{EOS}} = 9.76688$, $\log_{10}(\tau_0/\mathrm{s}) = -9.51554$, $A = 311.84511$ cm$^{3\gamma}$ g$^{-\gamma}$ K, $D = 4.19154$, $\gamma = 1.02184$.

[42] M. Naoki, H. Endou, and K. Matsumoto, J. Phys. Chem. **91**, 4169 (1987).

[43] See Supplemental Material at http://link.aps.org/supplemental/10.1103/PhysRevLett.115.265702, which includes Refs. [44,45], for a comparison of the slopes of the confined liquid data and extrapolated to negative pressure isochores, as well as additional results for van der Waals liquid dimethyl phthalate.

[44] K. Adrjanowicz, A. Grzybowski, K. Grzybowska, J. Pionteck, and M. Paluch, Cryst. Growth Des. **14**, 2097 (2014).

[45] The fitting parameters for dimethyl phthalate are $\log_{10}(\tau_0/\mathrm{s}) = -10.90$, $A = 153.61$ cm$^{3\gamma}$ g$^{-\gamma}$ K, $D = 3.501$, and $\gamma = 3.93$.

[46] W. K. Kipnusu, M. Elsayed, W. Kossack, S. Pawlus, K. Adrjanowicz, M. Tress, E. U. Mapesa, R. Krause-Rehberg, K. Kaminski, and F. Kremer, J. Phys. Chem. Lett. **6**, 3708 (2015).

[47] S. P. Andersson and O. Andersson, Macromolecules **31**, 2999 (1998).